# Immunological profiles of human oligodendrogliomas define two distinct molecular subtypes

Fan Wu,[a,b,c,d,**] Yi-Yun Yin,[a,b,c,d] Wen-Hua Fan,[a,b,c,d] You Zhai,[a,b,c,d] Ming-Chen Yu,[a,b,c] Di Wang,[a,b,c] Chang-Qing Pan,[a,b,c] Zheng Zhao,[a,b,c] Guan-Zhang Li,[a,b,c] and Wei Zhang[a,b,c,*]

[a]Department of Molecular Neuropathology, Beijing Neurosurgical Institute, Capital Medical University, Beijing, 100070, China
[b]Department of Neurosurgery, Beijing Tiantan Hospital, Capital Medical University, Beijing, 100070, China
[c]Chinese Glioma Genome Atlas Network (CGGA) and Asian Glioma Genome Atlas Network (AGGA), Beijing, 100070, China

## Summary

**Background** Human oligodendroglioma presents as a heterogeneous disease, primarily characterized by the isocitrate dehydrogenase (*IDH*) mutation and 1p/19q co-deletion. Therapy development for this tumor is hindered by incomplete knowledge of somatic driving alterations and suboptimal disease classification. We herein aim to identify intrinsic molecular subtypes through integrated analysis of transcriptome, genome and methylome.

**Methods** 137 oligodendroglioma patients from the Cancer Genome Atlas (TCGA) dataset were collected for unsupervised clustering analysis of immune gene expression profiles and comparative analysis of genome and methylome. Two independent datasets containing 218 patients were used for validation.

**Findings** We identified and independently validated two reproducible subtypes associated with distinct molecular characteristics and clinical outcomes. The proliferative subtype, named Oligo1, was characterized by more tumors of CNS WHO grade 3, as well as worse prognosis compared to the Oligo2 subtype. Besides the clinicopathologic features, Oligo1 exhibited enrichment of cell proliferation, regulation of cell cycle and Wnt signaling pathways, and significantly altered genes, such as *EGFR*, *NOTCH1* and *MET*. In contrast, Oligo2, with favorable outcome, presented increased activation of immune response and metabolic process. Higher T cell/APC co-inhibition and inhibitory checkpoint levels were observed in Oligo2 tumors. Finally, multivariable analysis revealed our classification was an independent prognostic factor in oligodendrogliomas, and the robustness of these molecular subgroups was verified in the validation cohorts.

**Interpretation** This study provides further insights into patient stratification as well as presents opportunities for therapeutic development in human oligodendrogliomas.

**Funding** The funders are listed in the Acknowledgement.

**Keywords:** Oligodendrogliomas; Molecular subtype; Immunological profiling; Prognosis; Multi-omics

## Introduction

According to the most recent World Health Organization (WHO) classification guidelines, oligodendroglioma, an incurable glioma, is characterized by mutations in *IDH1* or *IDH2* and co-deletion of chromosome arms 1p and 19q.[1,2] Accounting for 4–8% of diagnosed primary tumors of the central nerve system (CNS), oligodendrogliomas can be divided into two groups based on the integrated histological and molecular features: CNS WHO grade 2 and grade 3.[3,4] This tumor shows relatively better prognosis among diffuse gliomas, ranging from a few years to more than 15 years.[5] It tends to be less aggressive and more sensitivity to radio and chemotherapy, but remains invariably fatal.[6] Recent high-throughput sequencing has also identified *FUBP1*, *CIC*, *TCF12*, and Telomerase reverse transcriptase (*TERT*) promoter mutations in the majority of this glioma.[7,8] Despite the described

**Research in context**

**Evidence before this study**
Although oligodendroglioma shows more sensitivity to normal therapies, it is an incurable brain tumor with high heterogeneity. Immunotherapy has made exciting progress in many malignant cancers, but yields very limited success in gliomas. To explore the immune heterogeneity and establish immune classification will facilitate the immunotherapies in oligodendroglioma.

**Added value of this study**
Here, using unsupervised clustering analysis based on immune-related gene expression profiles, we classified oligodendrogliomas into two distinct subtypes. The stability and reproducibility of this classification were demonstrated in other two independent datasets. Each subtype was associated with different somatic alterations, immune cells, and metabolic features, as well as clinical outcomes. Oligo1

subtype displayed a proliferative phenotype and higher mutation frequency in *EGFR*, *MET* and *NOTCH1*. Oligo2 subtype, with better outcome, presented an immune suppressive status and had higher metabolic activities. The distinct features between them implied different therapeutic strategies, and immunotherapies targeting at inhibitive checkpoints might be effective in Oligo2 tumors.

**Implications of all the available evidence**
This study reported a new immune classification of oligodendrogliomas and comprehensively characterized the identified subtypes with genome and methylome data, which deepened the understanding of immune heterogeneity of human oligodendroglioma, and provided valuable information for personalized immune-targeted therapy in this tumor entity.

molecular advances, our understanding of the biology and molecular mechanisms underlying the behavior of oligodendrogliomas is extremely limited.

Recent evidence shows that oligodendrogliomas are heterogeneous in terms of clinical, histological, and molecular profiles, and many efforts have been devoted to identifying subgroups through multi-omics analysis. Comparative analysis showed that the rate of shared mutation between the primary and recurrent oligodendrogliomas was relatively low, ranging from 3.2 to 57.9%, indicating high genetic heterogeneity.[8] Single cell transcriptome of oligodendrogliomas found that most tumor cells were differentiated along two specialized glial programs, whereas a rare subpopulation of cells was undifferentiated and associated with a neural stem cell expression program, demonstrating the intratumoral heterogeneity.[9] An integrated analysis of transcriptome, genome and methylome revealed three subgroups within 1p/19q co-deleted tumors, and one group was associated with more aggressive clinical and molecular patterns, including the *MYC* pathway activation.[10] However, our knowledge about molecular characteristics and subtypes of oligodendrogliomas is incomplete.

Numerous studies have explored the classification of tumors based on immunological profiling that may facilitate the optimal stratification of cancer patients responsive to immunotherapy. An extensive immunogenomic analysis of more than 10,000 tumors comprising 33 diverse cancer types identified six immune subtypes: wound healing, IFN-γ dominant, inflammatory, lymphocyte depleted, immunologically quiet, and TGF-β dominant.[11] Based on the immune gene expression profiles of 1368 squamous cell carcinomas patients, six reproducible immune subtypes associated with distinct molecular characteristics and

clinical outcomes were obtained.[12] In an analysis of hepatocellular carcinomas samples from 956 patients, two subclasses were characterized by adaptive or exhausted immune responses.[13] Through immunogenomic profiling of 29 immune signatures, three triple-negative breast cancer subtypes that named immunity high, medium, and low were identified.[14] In gliomas, we previously gathered published gene expression data from diffuse lower-grade glioma (LGG) patients and uncovered three immune subtypes characterized by differences in somatic alterations, lymphocyte signatures, and clinical outcomes.[15] Three glioblastoma (GBM) subgroups presented different adaptive immune responses: Negative, Humoral, and Cellular-like, and were linked to transcriptional subtypes and typical genetic alterations.[16] Gene signatures of infiltrating immune cells and functional immune pathways clustering revealed four distinct immune clusters: vascular, monocytic/stromal, monocytic/T cell- and APC/NK/T cell-dominant in pediatric and adult high-grade gliomas.[17] However, little is known regarding tumor microenvironment (TME) heterogeneity and immune groups in oligodendrogliomas.

Immunotherapy has been explored as a potential treatment modality in gliomas. Numbers of immunotherapeutic strategies have been evaluated in various preclinical and clinical studies of glioblastoma, but exhibit limited efficacy, such as immune checkpoint inhibitors, cytokine, dendritic cell vaccines, chimeric antigen receptor T cells (CAR-T).[18,19] For low-grade gliomas (LGGs) or oligodendrogliomas, checkpoint inhibitors, polyinosinic polycytidylic acid stabilized lysine, and carboxymethylcellulose (poly-ICLC), peptide vaccines, such as a vaccine targeting mutant *IDH1*,[20,21] are being assessed, but few immunotherapies have demonstrated a robust survival impact in clinical trials.

LGGs or oligodendrogliomas may have unique tumor immune phenotypes, with their *IDH* mutations potentially making them less vulnerable to specific types of immunotherapies. A better understanding of immune microenvironment and molecular subtypes may provide a solid basis for the scientific design and reasonable choice of immunotherapeutic strategies in oligodendrogliomas.

Here, using unsupervised clustering analysis based on immune-related gene expression profiles, we classified oligodendrogliomas into two distinct subtypes. We demonstrated the stability and reproducibility of this classification in other two independent datasets. Each subtype was associated with different somatic alterations, immune cells, and metabolic features, as well as clinical outcomes. Our analysis uncovered the heterogeneity of oligodendrogliomas in aspect of immunity, setting the ground for a rational tailoring of immunotherapy in patients.

## Methods

### Patients and datasets

This study gathered 355 oligodendrogliomas from three public databases: TCGA, Chinese Glioma Genome Atlas (CGGA), and Prise en charge des oligodendrogliomas anaplasiques (POLA). For the discovery cohort, the RNA-seq data, DNA methylation data, somatic alterations, and corresponding clinical information of 137 oligodendroglioma patients were collected from TCGA database (http://cancergenome.nih.gov).[22] The RNA-seq data and clinical information of 124 samples were downloaded from CGGA database (http://www.cgga.org.cn) for the validation cohort.[23,24] For another validation cohort, the microarray data, DNA methylation data, and related clinical information of 94 oligodendroglioma samples were obtained from POLA database.[10] A summary of patients of the tumor cohorts and respective pathological features was listed in Supplementary Table S1. All patient informed and written consents were previously existed in these three databases.

### Ethics approval and consent to participate

This study was carried out in accordance with the Helsinki declaration and approved by the ethics committee of Tiantan hospital (KYSQ 2021-309-01), and patient informed consents were existed in these three public databases.

### Discovery and validation of the immune subtypes

The published immune-related genes were gathered for subsequent clustering analysis.[25,26] Genes significantly associated with prognosis were identified using survival analysis in the TCGA cohort with R package "survival". Then, the candidate genes with high median absolute deviation (MAD) value (MAD $\geq$ 0.5) across all patients were adopted for consensus clustering analysis (R package "consensusClusterplus").[27,28] To identify robust clusters, the cumulative distribution function (CDF) and consensus heatmap were used to evaluate the optimal K. For the validation of the immune subtypes in other cohorts, a partition around medoids (PAM) classifier was trained and used to predict immune subtypes for patients with R package "pamr". Each sample was assigned to an immune subtype based on the Pearson correlation with the centroid.[29,30] The reproducibility and similarity of acquired immune subtypes between the discovery and validation cohorts were assessed using the in-group proportion (IGP) statistic with R package "clusterRepro".[31]

### Computation of immune infiltration

CIBERSORT algorithm was adopted to estimate the relative fraction of 22 immune cell types.[32,33] ESTIMATE was used to evaluate the immune cell and stromal content for each sample.[34] Single-sample gene-set enrichment analysis (ssGSEA) was performed to quantify the enrichment levels of immune signatures with R package "GSVA".[14,35]

### Computation of metabolism-relevant gene signatures

115 metabolism-relevant gene signatures were acquired from previously published studies.[36,37] By using R package "GSVA", the enrichment levels of metabolism-relevant signatures were quantified for each sample.

### Bioinformatic analysis

Principal components analysis (PCA) was applied to detect the expression difference between subtypes (R package "princomp").[38] Receiver-operating characteristic (ROC) curve analysis was conducted to predict overall survival (OS) (R package "pROC"). Gene ontology (GO) analysis was used for functional annotation of differential genes between subtypes.[39] GISTIC2.0 analysis was performed to detect copy number alterations (CNAs) difference between subtypes,[40] and locus with GISTIC value more than 1 or less than −1 was defined as amplification or deletion, respectively.

### Cell lines and culturation

LN229 and GL261 cells were obtained from American Type Culture Collection (ATCC, Rockville, MD), and were maintained in Dulbecco's modified Eagle's medium (DMEM) with high glucose and sodium pyruvate supplemented with 10% foetal bovine serum (FBS) and 1% Penicillin-Streptomycin. These cell lines had been performed short tandem repeat (STR) profiling analysis

and tested negative for mycoplasma contamination (Reagent Validation Files).

### Cell viability assay

Cell viability was determined using cell counting kit-8 (CCK-8) assay (ab228554, Abcam, Burlingame, CA, USA). 3000 cells per well were seeded in a 96-well plate, and treated with 10 uM Gefitinib (ZD1839, MedChemExpress, NJ, USA), or 10 uM Crizotinib (PF-02341066, MedChemExpress, NJ, USA). At 0 h, 24 h, and 48 h, the CCK8 regent was added and incubated for 60 min at 37 °C, the absorbance (OD value) was detected at a wavelength of 450 nm.

### Western blotting

Protein extraction and Western blot analysis were performed as described previously.[41] Antibodies used were as followed: anti-p-MET (3077, 1:1000, RRID: AB_2143884, Cell Signaling, Danvers, Massachusetts, USA), anti-p-EGFR (3777, 1:1000, RRID: AB_2096270, Cell Signaling), and anti-GAPDH (60004-1-lg, 1:3000, RRID: AB_2107436, Proteintech, Wuhan, Hubei, PR China). All antibodies were validated by the commercial vendor.

### T cell and monocyte cell migration assay

Human T cells were isolated from peripheral blood of normal donors using T cell Isolation Kit (130-096-535, Miltenyi, Germany) and cultured in RPMI 1640 medium supplemented with 10% FBS, 20 mM HEPES and 50 U/ml interleukin-2 (200-02, Peprotech, USA). $1 \times 10^5$ T cells were seeded into the upper chamber with 5 um pore (Corning, USA), and LN229 cells treated with 10 uM Gefitinib or 1 uM Crizotinib for 12 h were maintained in the lower chamber. After 8-h coculturation, the migrated T cells were counted. THP-1 cells were obtained from American Type Culture Collection (ATCC, Rockville, MD) and cultured in RPMI 1640 medium supplemented with 10% FBS and 0.1 ug/ml PMA (HY-18739, MedChemExpress, NJ, USA). $1 \times 10^5$ THP-1 cells were seeded into the upper chamber with 8 um pore (Corning, USA) and cocultured with LN229 cells. After 8-h incubation, the migrated cells at the bottom surface were fixed and stained with 0.1% crystal violet. 6 random fields in each well were counted.

### Xenograft studies and treatment experiments

$1 \times 10^6$ GL261 cells stably expressing the luciferase reporter were stereotactically injected into the right striatum of 6-week-old, female, C57BL/6J mice. After a week, the mice were imaged for Fluc activity using bioluminescence imaging through 10 ul/g D-luciferin injection, and randomly assigned to treatment groups of

Gefitinib (oral administration, 100 mg/kg), Crizotinib (oral administration, 50 mg/kg), and vehicle control. Animals were treated daily for five days, followed by two days of rest. The tumor size was detected with bioluminescence imaging, and the survival information was recorded. Mice with severe symptoms including dome head and hemiparesis were euthanized, and the brains were fixed in 4% paraformaldehyde and embedded for the following staining analysis. All animal care and experimental procedures were approved by the Animal Care and Use Committee of Tiantan hospital (VST-SY-20220712).

### Immunohistochemical staining

Paraffin-embedded tissues of 24 cases from CGGA cohort were collected for immunohistochemical staining (Supplementary Table S2). In brief, the sections were incubated with antibodies overnight at 4 °C, and then with secondary antibodies at room temperature for 1 h. After staining with DAB (MXB, Fuzhou, Fujian, PR China) for 1min, sections were counterstained with hematoxylin (Solarbio, Tongzhou, Beijing, PR China). The used antibodies included anti-CD163 (16646-1-AP, 1:300, RRID: AB_2756528, Proteintech, Wuhan, Hubei, PR China) and anti-CD206 (18704-1-AP, 1:300, RRID: AB_10597232, Proteintech) for M2 macrophages, anti-CD3 (ab16669, 1:300, RRID: AB_443425, Abcam, Burlingame, CA, USA) for lymphocytes, anti-CD14 (ab183322, 1:300, RRID: AB_2909463, Abcam) for monocytes, anti-TIGIT (99567, 1:300, RRID: AB_2922806, Cell Signaling, Danvers, Massachusetts, USA), anti-HAVCR2 (60355-1-1g, 1:300, RRID: AB_2881464, Proteintech), anti-MET (8198, 1:300, RRID: AB_10858224, Cell Signaling), anti-EGFR (4267, 1:300, RRID: AB_2246311, Cell Signaling), anti-NOTCH1 (20687-1-AP, 1:300, RRID: AB_10700012, Proteintech). All antibodies were validated by the commercial vendor. Six fields of each section were selected for quantitative analysis, and stained cells were counted by two investigators independently.

### Statistical analysis

Kaplan–Meier analysis with log-rank test was conducted to detect survival difference between subtypes. For comparisons of two groups, statistical significance for normally distributed variables was estimated by unpaired Student $t$-test, and nonnormally distributed variables were analyzed by Wilcon rank-sum test. The Benjamini-Hochberg method was used to adjust the $P$ value. Chi-square test was performed to determine the difference of clinical and molecular characteristics between subtypes. For univariable analysis, we selected factors known to impact outcomes as well as patient characteristics.[22,42,43] The clinical characteristics of patients (Supplementary Table S1) showed that *MGMT*

promoter is methylated in almost all patients, and *TERT* promoter status is mostly unavailable in three datasets. So, age, sex, and grade were included for subsequent Cox analysis. We used Cox proportional hazards model to examine the effects of these different risk factors on event outcomes. Schoenfeld residual was used to assess the reliability of the model. Cox multivariable analysis was performed to adjust for explanatory confounding variables prognostic on univariable analysis. All statistical analyses were performed with R software, Graph-Pad Prism 6.0 (GraphPad Inc., San Diego, CA, USA) or SPSS 16.0 (IBM, Chicago, IL, USA). $P < 0.05$ was considered statistically significant.

### Role of funders
The funders only provided funding, and had no role in the study design, data collection, data analysis, decision to publish, or preparation of the manuscript.

## Results
### Consensus clustering reveals two distinct tumor subgroups in oligodendrogliomas
To delineate the immune heterogeneity within oligo-dendrogliomas, we gathered previously reported 782 immune-relevant genes for clustering analysis.[25,26] Fig. 1a showed the workflow of this study. We first conducted survival analysis to identify genes with prognostic significance, and a total of 84 candidate genes were acquired for subsequent clustering analysis in the TCGA cohort. Through unsupervised consensus clustering analysis, two immune subtypes, Oligo1 and Oligo2, were identified (Fig. 1b and Supplementary Fig. S1). We performed PCA to assess the assignments of subtypes, and further confirmed the robust difference of expression patterns between subtypes (Fig. 1c). Next, we determined the correlation of subtypes with molecular and pathological characteristics. The statistical analysis (Chi-square test) found that histologic grade 3 was associated with Oligo1 subtype, and patients in Oligo1 tended to be older than ones in Oligo2 (Fig. 1b, Supplementary Table S3). We also compared our classification with the previously reported immune subtyping of gliomas,[11] and found that most of Oligo1 and Oligo2 tumors were enriched in C5 cluster (Supplementary Fig. S2a). Notably, survival analysis showed that Oligo1 subtype likely had a worse outcome compared to Oligo2 subtype ($P$ = 0.0041, log-rank test) (Fig. 1d), and the resulting classification was significantly associated with overall survival, independent of other clinicopathological features (Supplementary Table S4). Besides, the developed grouping had higher AUC compared with factor of histologic grade (Supplementary Figs. S2b and S2c), which implied its superior performance of prognosis prediction.

### Validation of immune subtypes across datasets
We evaluated the reproducibility and robustness of the immune subtypes in two additional cohorts. The centroid of each immune subtype was calculated, and each sample in validation cohorts was assigned to a subtype according to the Pearson correlation of centroid[29] (Fig. 2a and d). Then, we performed IGP statistical analysis and found high concordance of gene expression patterns between discovery and validation cohorts (Supplementary Table S5). PCA also confirmed the expression profile difference between acquired immune subtypes (Fig. 2b and e). Consistently, Oligo1 mainly consisted of CNS WHO grade 3 and older patients, and was associated with a shorter overall survival in CGGA cohort ($P$ = 0.021, log-rank test) (Fig. 2c, Supplementary Table S6). Likewise, the immune classification presented higher AUC than factor of grade, which could not clearly distinguish patients' outcomes (Supplementary Fig. S2d and S2e). Univariable and multivariable Cox regression analyses also demonstrated that this stratification was of prognostic significance in CGGA cohort (Supplementary Table S7). In the POLA cohort, Chi-square test showed grade 3 was significantly associated with Oligo1 subtype (Supplementary Table S8). Due to the limited follow-up, and median overall survival was not reached (Fig. 2f), it was difficult to assess the correlation between the acquired classification and patients' outcome (Supplementary Table S9). We also performed the subtyping of grade 2 and grade 3 tumors in TCGA and CGGA cohorts, and found that our classification likely differentiated the outcome in patients of CNS WHO grade 2 (TCGA cohort), grade 2 and grade 3 (CGGA cohort) (Supplementary Fig. S3).

### Somatic variations of immune subtypes
Numerous studies have revealed the close connection between somatic alterations and immune infiltrates.[11,44] We further explored somatic variations that might drive the immune subtypes potentially. The genomic alteration data from TCGA cohort was enquired and the correlations of immune subtypes with somatic drivers were examined. Oligo1 tumors showed higher aneuploidy, tumor mutation burden, and copy number burden scores (Fig. 3a). The statistical analysis was performed with the Fisher test (Supplementary Table S10), and the genes with high mutation frequency were shown in Fig. 3b. *EGFR* alterations were significantly enriched in Oligo1 samples, whereas most of common gene variations showed nonspecific association between subtypes, such as *CIC*, *FUBP1*, and *RB1*. Then, the differentially enriched genes were functionally annotated with GO analysis (Supplementary Fig. S4a), and the specific altered genes of Oligo1 tumors were mainly enriched in Wnt signaling pathway, regulation of neurogenesis, and semaphorin-plexin
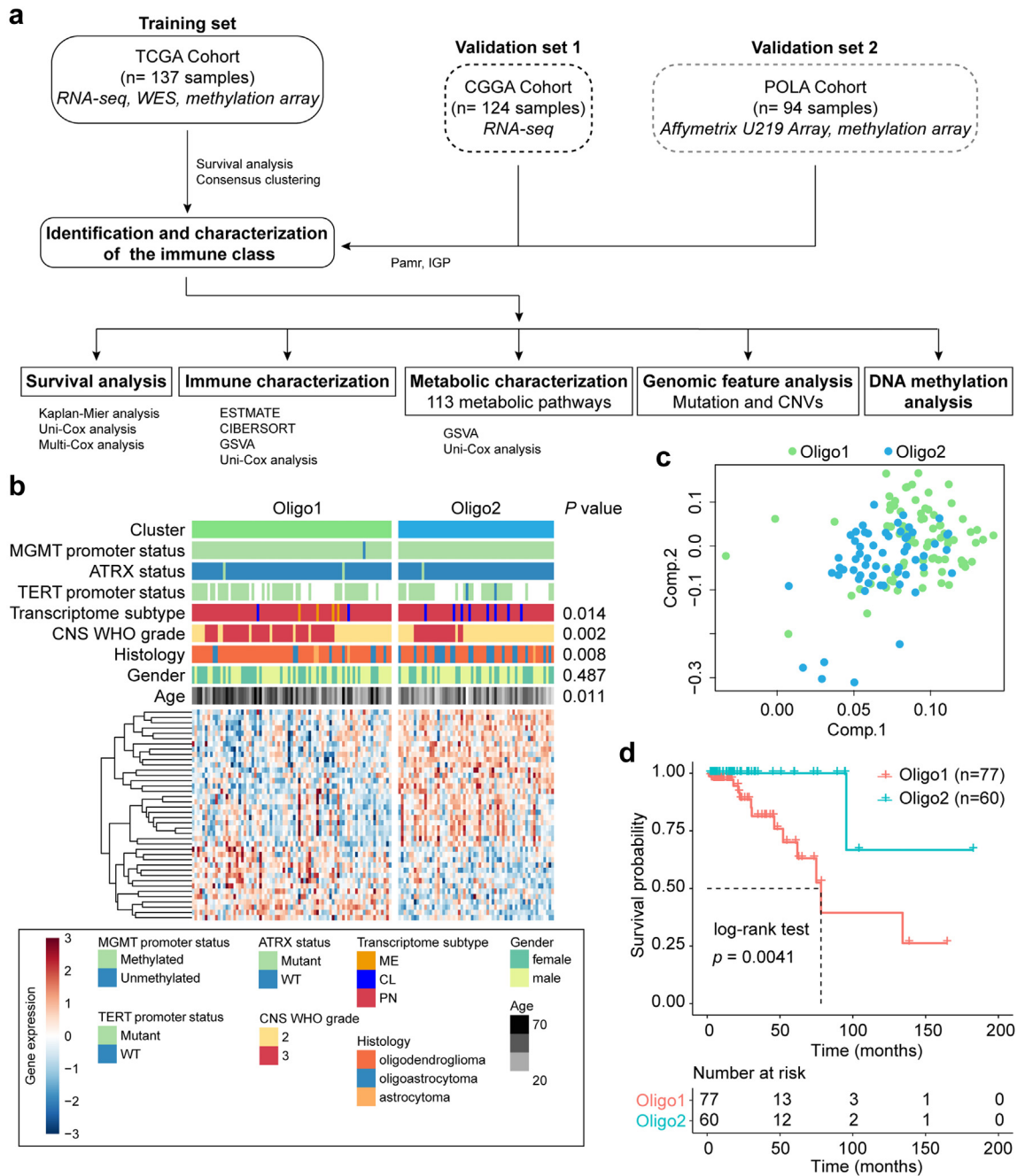
**Fig. 1: Immune gene profile of oligodendrogliomas yields two subtypes in TCGA cohort. a** Flow chart of this study. A total of 355 oligodendroglioma samples are used in this study. TCGA cohort is used as training set, CGGA and POLA cohorts are collected as validation sets. **b** Heatmap of two immune subtypes defined in TCGA cohort. 40 genes of centroid derived from PAM classifier are showed. Patients are arranged based on the subtypes. Molecular and clinical information are also annotated for each patient. CL, classical; MES, mesenchymal; PN, proneural. **c** Principal component analysis (PCA) of two subtypes using whole transcriptome data. **d** Survival analysis of immune subtypes based on OS. *P* value is calculated by the log-rank test between subtypes.

pathway (Fig. 3b). Consistently, the expression of amplificated genes (*EGFR* and *MET*) were higher in Oligo1 than in Oligo2 tumors (Supplementary Fig. S4b).

Immunohistochemical staining also confirmed the increased *MET* and *EGFR*, and decreased *NOTCH1* protein levels in Oligo1 (Supplementary Fig. S4c).
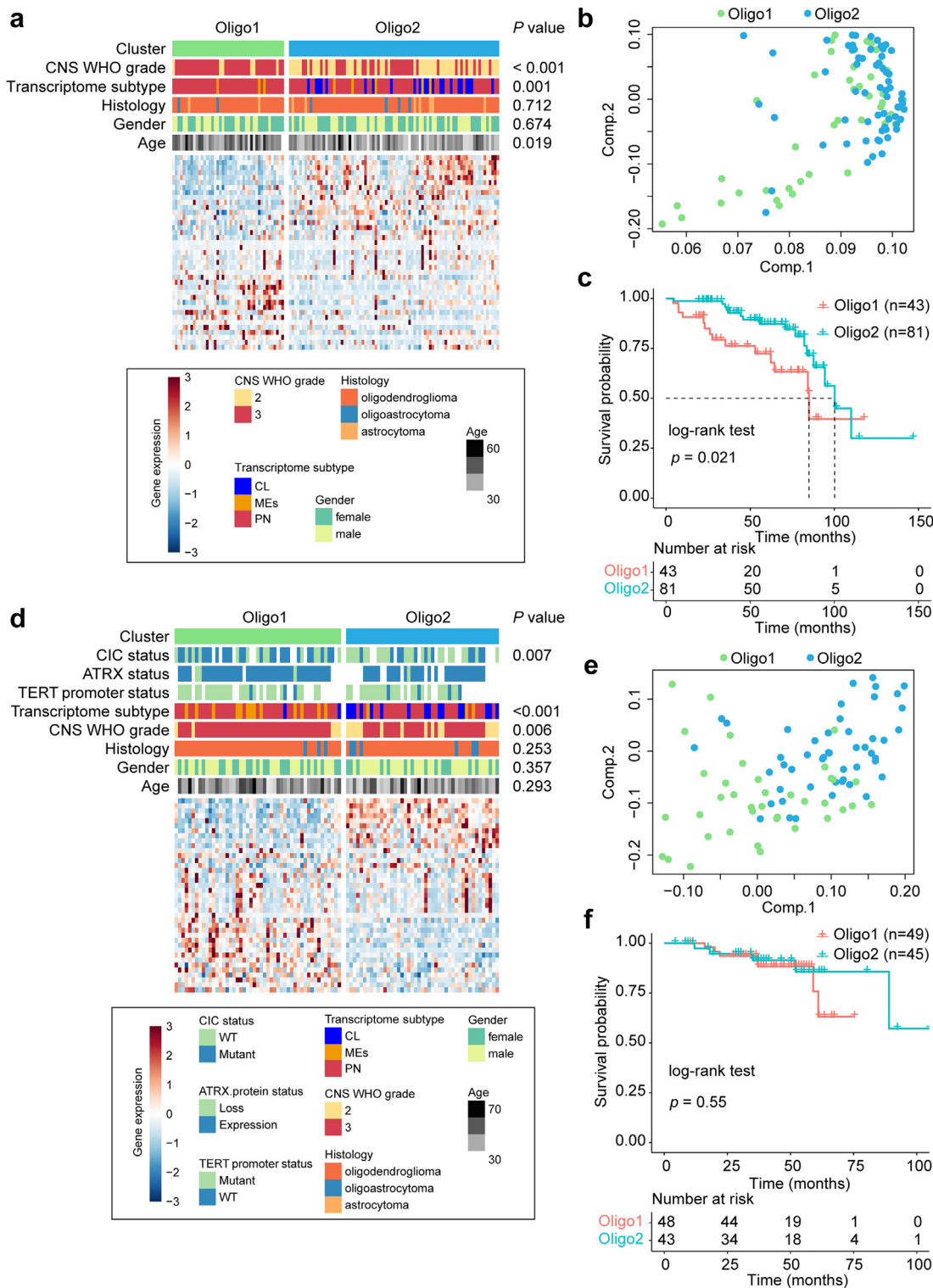
**Fig. 2: External validation of the immune class in the publicly available CGGA and POLA datasets. a** Heatmap shows the immune subtypes of CGGA cohort predicted by a PAM classifier trained on the TCGA cohort. Patients are arranged based on the predicted immune subtypes. The 40 centroid genes and clinical information are displayed. CL, classical; MES, mesenchymal; PN, proneural. **b** Principal component analysis (PCA) of two subtypes using whole transcriptome data in CGGA cohort. **c** The Kaplan–Meier analysis (log-rank test) of immune subtypes based on OS.
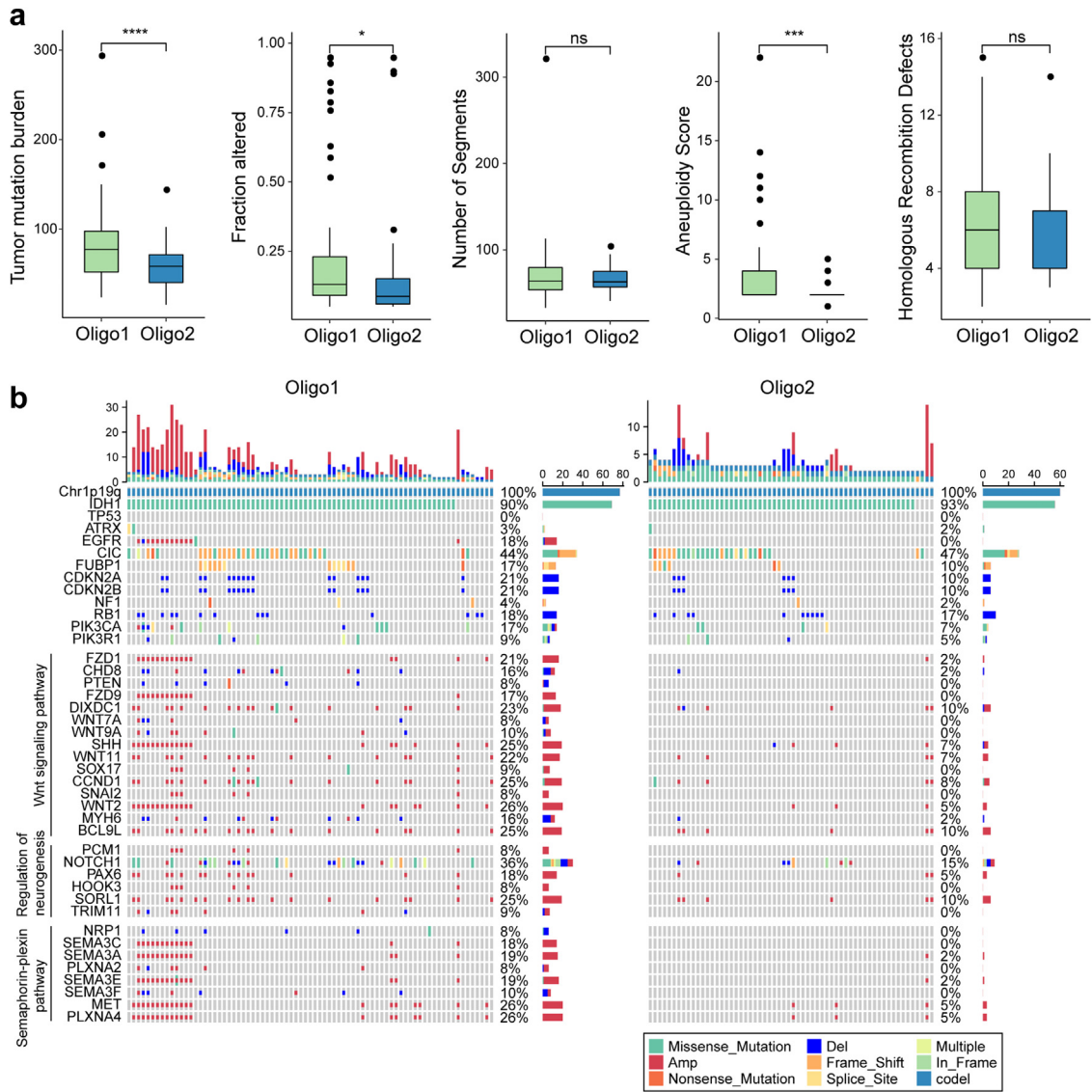
*Fig. 3:* **Comparison of the DNA alterations between immune subtypes in TCGA cohort. a** Boxplots show the difference of DNA damage measures between subtypes of TCGA cohort (Wilcon rank-sum test). Error bars show standard error of the mean, and the middle bar represents the median level of corresponding features. *$P < 0.05$, ***$P < 0.001$ **b** Oncoprint of mutation status and copy number variations between immune subtypes. Fisher test is adopted for comparison analysis. The differentially altered genes annotated to Wnt signaling, regulation of neurogenesis, and semaphorin-plexin pathway are displayed.

## DNA methylation changes in the immune subtypes

To better understand epigenetic differences between Oligo1 and Oligo2 subtypes, we investigated the differentially methylated CpG sites of these samples from TCGA cohort. 1601 CpG probes were differentially methylated between subtypes. We ranked the probe list by decreasing beta-value difference in order to identify the most top differentially CpG probes (Fig. 4a). Genes with methylation changes in Oligo1 tumors were highly enriched for cell proliferation, Wnt signaling pathway, chemical synaptic transmission, and signal transduction (Fig. 4b). In addition, the differentially methylated genes

**d** Heatmap shows the immune subtypes of POLA cohort predicted by a PAM classifier trained on the TCGA cohort. The 40 centroid genes and clinical information are also displayed. **e** PCA of immune subtypes using whole transcriptome data in POLA cohort. **f** Survival analysis of immune subtypes in POLA cohort. *P* value is calculated by the log-rank test between subtypes.
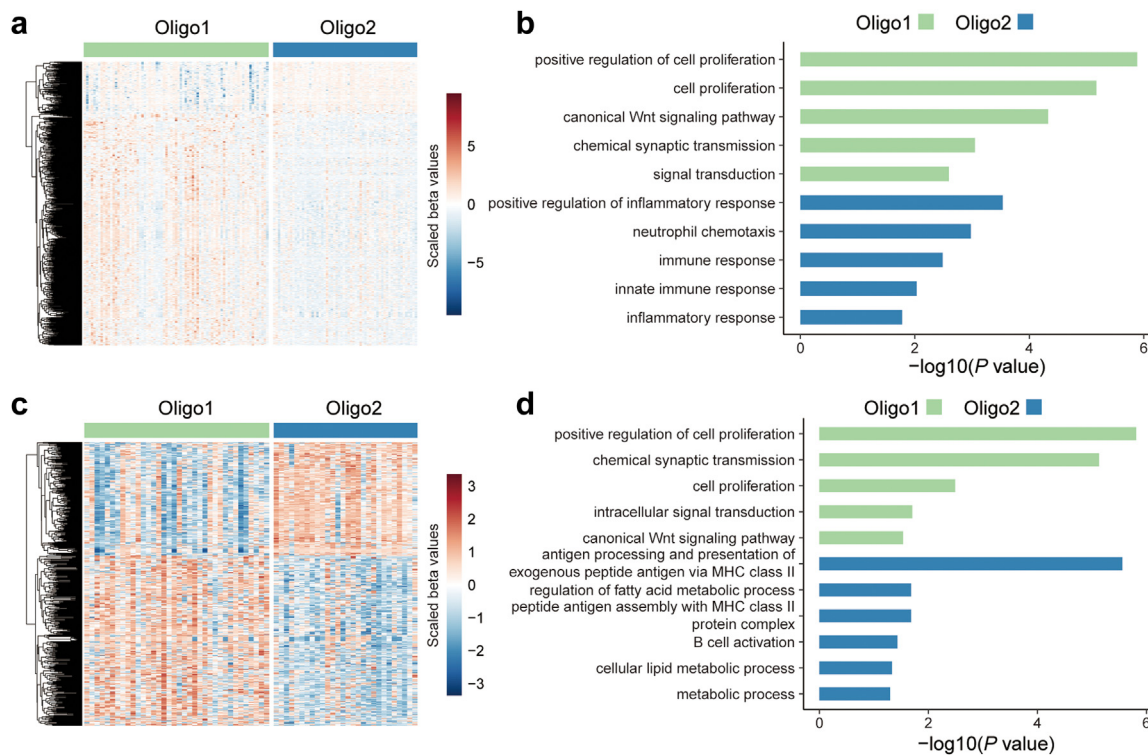
**Fig. 4: Comparison of the DNA methylation between subtypes in TCGA and POLA cohorts. a** Heatmap of TCGA samples ordered according to subtypes using the top differential 637 probes defined by Wilcoxon test. **b** Gene Ontology (GO) analysis of the differentially methylated genes between subtypes in TCGA cohort. **c** Heatmap of POLA samples ordered according to subtypes using the top differential 500 probes defined by Wilcoxon test. **d** Functional annotation of the differentially methylated genes between subtypes in POLA cohort.

in Oligo2 tumors were highly enriched among functional categories involved in immune response and inflammatory response (Fig. 4b). To extend these findings, the DNA methylation data from POLA cohort (64 samples available) was also enquired, and similar results were obtained (Fig. 4c and d). The differentially methylated genes in Oligo2 tumors were associated with antigen processing and presentation, metabolism process, and B cell activation (Fig. 4d).

**Transcriptome analysis of the immune subtypes**
Next, we analyzed the functional context of these two subtypes with transcriptome data of TCGA cohort. Gene ontology (GO) analysis based on the differentially expressed genes between subtypes, which were identified with R package "samr" (FDR <0.05, student *t*-test), showed the highly expressed genes in Oligo1 were mainly enriched in chemical synaptic transmission, neurotransmitter secretion, Wnt signaling pathway, regulation of cell cycle, and G2/M transition of mitotic cell cycle. Instead, the upregulated genes in Oligo2 were annotated to antigen processing and presentation, oxidation-reduction process, metabolic process, and

innate immune response (Supplementary Fig. S5a and S5b). These functional analyses were then repeated on the CGGA and POLA cohorts, and GO also reproduced the enriched functions of these two immune subtypes (Supplementary Fig. S5c–S5f).

**Cellular and molecular characteristics of immune subtypes**
Due to the significant difference in immune-related functions between subtypes, we resorted to several previously reported immune-related tools to decipher the immune infiltration of immune subtypes. We first determined the stromal and immune scores by computing the ESTIMATE algorithm.[34] Compared with Oligo1, Oligo2 subtype showed higher immune and stromal scores (Fig. 5a). Then, we explored the composition of infiltrating immune cells between groups by CIBERSORT method.[32] Oligo1 had increased percentage of lymphocytes and plasma cells, whereas Oligo2 displayed higher level of macrophages and monocytes (Fig. 5b and c). Additionally, ssGSVA scores[35] were adopted to quantify the enrichment levels of immune cells and functions. Oligo2 showed increased functions
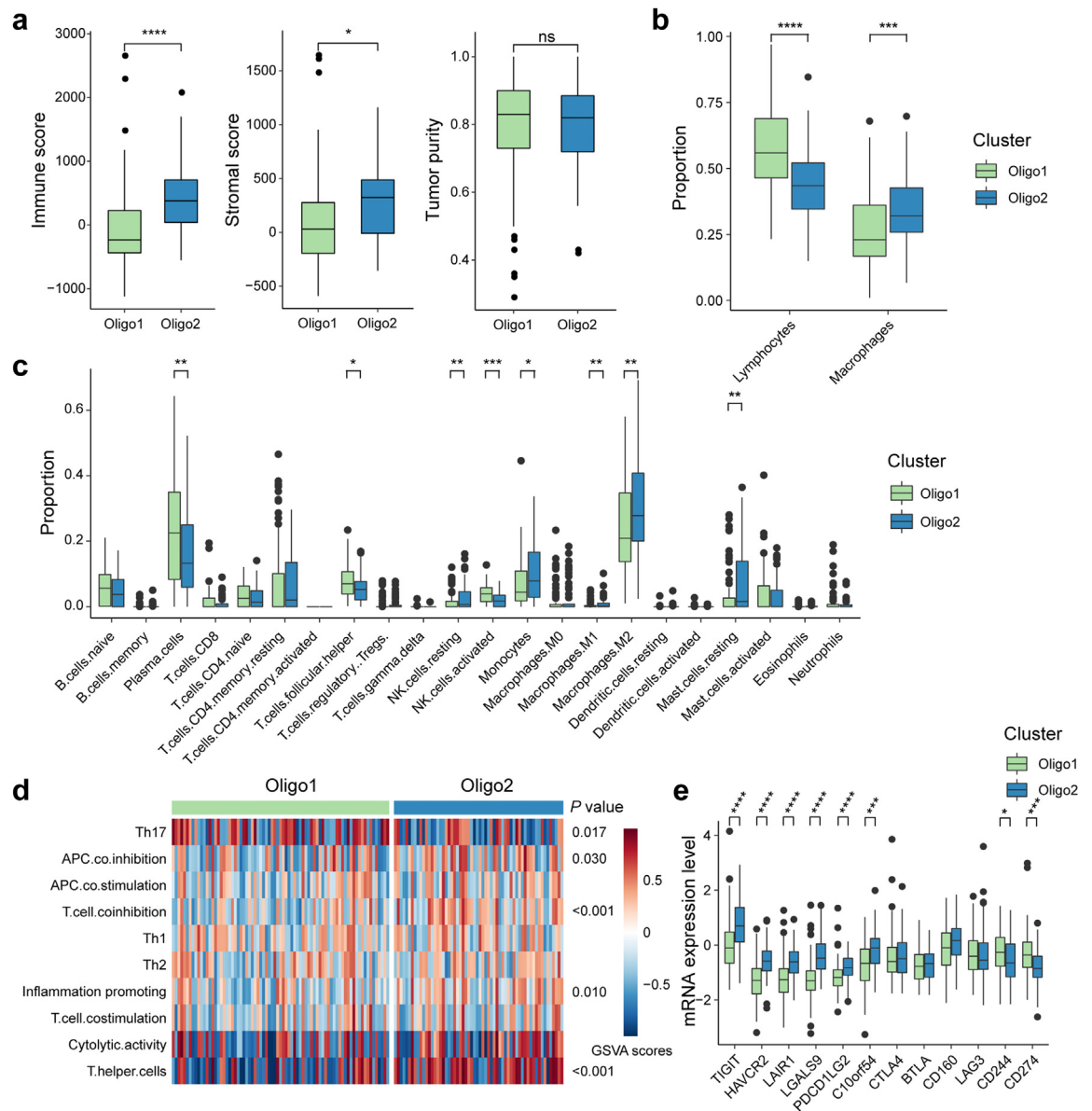
Fig. 5: Tumor immune infiltration dissection of two subtypes in TCGA cohort. **a** Comparison of immune, stromal, and tumor purity scores from ESTIMATE for immune subtypes (Wilcon rank-sum test). **b** Comparison of lymphocytes and macrophage proportion (from CIBERSORT) for immune subtypes (Wilcon rank-sum test). Lymphocytes consist of B cells, CD4 cells, CD8 cells, follicular helper T cells, Tregs, gamma delta T cells, NK cells, and plasma cells. **c** Relative abundance fractions of the immune cell population in two subtypes using CIBERSORT tool. **d** Heatmap shows enrichments of immune-related signatures in two immune subtypes. *P* values are labelled. **e** Boxplots display the expression levels of inhibitive checkpoint genes. *P < 0.05, **P < 0.01, ***P < 0.001, ****P < 0.0001, Wilcon rank-sum test.

of APC and T-cell co-inhibition (Fig. 5d). Moreover, we detected the expression levels of several inhibitive checkpoint genes, since T cell and natural killer cell inhibition has been known as an important mechanism by which cancer cells escape immunity.[45,46] We observed that most of checkpoint genes, such as *TIGIT*, *HAVCR2, LAIR1, LGALS9, PDCD1LG2,* and *C10orf54*, were highly expressed in Oligo2 tumors (Fig. 5e),

indicating an elevated level of immunosuppression in these tumors. To validate these findings, we sought to dissect the immune infiltrations of each subtype in CGGA and POLA cohorts, and similar results were obtained (Supplementary Fig. S6, Supplementary Table S11). Immunohistochemical staining with tissues from CGGA cohort also confirmed our above findings using antibodies (CD206 and CD163 for M2
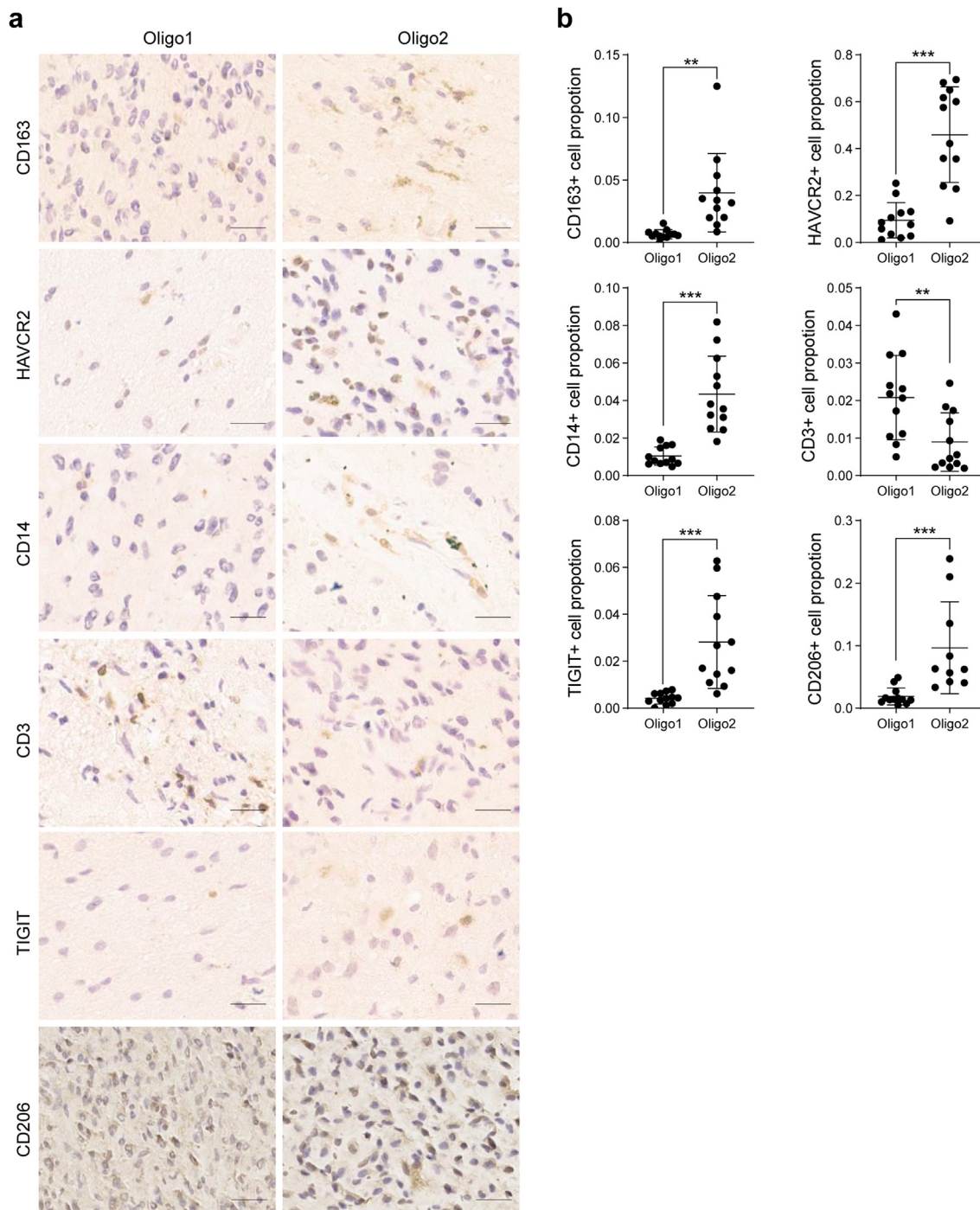
Fig. 6: **Immunostaining analyses of immune cells and checkpoints between subtypes. a** 12 Oligo1 and 12 Oligo2 cases were collected from CGGA cohort. NOTCH1, TIGIT, HAVCR2, CD206, CD163, CD14, and CD3 antibodies were used to assess cell proportions. **b** Boxplots shows the positive cell proportion evaluated by immunostaining. Scaled bar, 50 μm **P < 0.01, ***P < 0.001, Student t-test.

macrophages, CD14 for monocytes, CD3 for lymphocytes, TIGIT and HAVCR2) (Fig. 6). Taken together, these results suggested that the TME of Oligo2 was highly immunosuppressive, whereas Oligo1 displayed relatively moderate immune microenvironment.
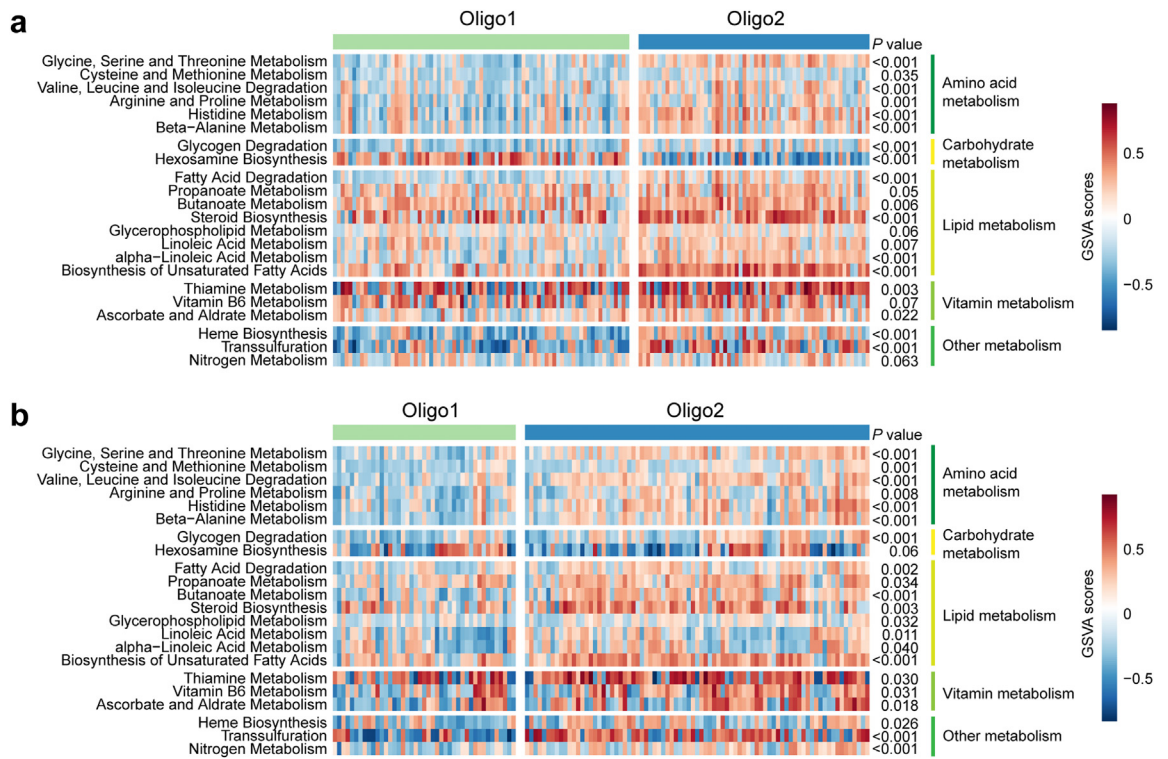
**Fig. 7:** Association between the acquired immune subtypes and metabolism-relevant signatures. **a** and **b** Heatmaps show the differential enrichments of metabolism-related signatures in the TCGA and CGGA cohorts. Amina acid, carbohydrate, lipid, vitamin, and other metabolism signatures are presented. The statistical difference is compared through the Wilcon rank-sum test, and the *P* value < 0.05 is considered significant.

## Metabolic profiling of the acquired immune subtypes

We further explored the metabolic characteristics of immune subtypes, in view of the enrichment difference of metabolic process identified by transcriptome analysis. GSVA was conducted to assess the enrichment levels of 115 metabolism-relevant gene signatures reported previously.[30,36] Differential analyses (Supplementary Table S12) showed that Oligo2 subtype displayed higher levels of metabolism processes that were related to amino acid, lipids, and vitamin. In contrast, Oligo1 tumors showed few enrichments of metabolism signatures, such as hexosamine biosynthesis, which indicated low metabolic activities (Fig. 7a). Next, we further interrogated CGGA and POLA cohorts and computed the metabolic scores, consistent findings were observed (Fig. 7b, Supplementary Fig. S7).

## Association between gene alterations and immune properties

Given the different immune and genomic properties between two molecular subtypes, we further enquired

the potential association between them. Since the oligodendroglioma cell line is lack and hard to be established, we chose glioblastoma cell lines LN229 (human) and GL261 (mouse) to validate our findings. Gefitinib and Crizotinib were used to inhibit *EGFR* and *MET* signal pathways, respectively. The p-MET and p-EGFR levels, and cell viability were reduced in the inhibitor treatment groups (Supplementary Fig. S8a and S8b). Then, T-cell and monocyte migration were assessed by cell co-culturation assays. LN229 cells treated with inhibitors showed decreased T-cell but stronger monocyte chemotaxis ability (Supplementary Figs. S9c and S8d).

We also performed in vivo assays to validate the immune-related functions of *MET* and *EGFR*. GL261 was intracranially injected, and the mice were treated with inhibitors after tumor formation. As shown in Supplementary Fig. S8e–S8g, *EGFR* and *MET* inhibition suppressed tumor growth and prolonged the survival of mice. IHC staining displayed tumors with inhibitor treatment had more CD14+ cells, TIGIT + cells, and CD206+ cells, but fewer CD3+ cells infiltration (Supplementary Fig. S9). These results indicated that *EGFR* and *MET* inhibition could impact the immune cell infiltration in gliomas.
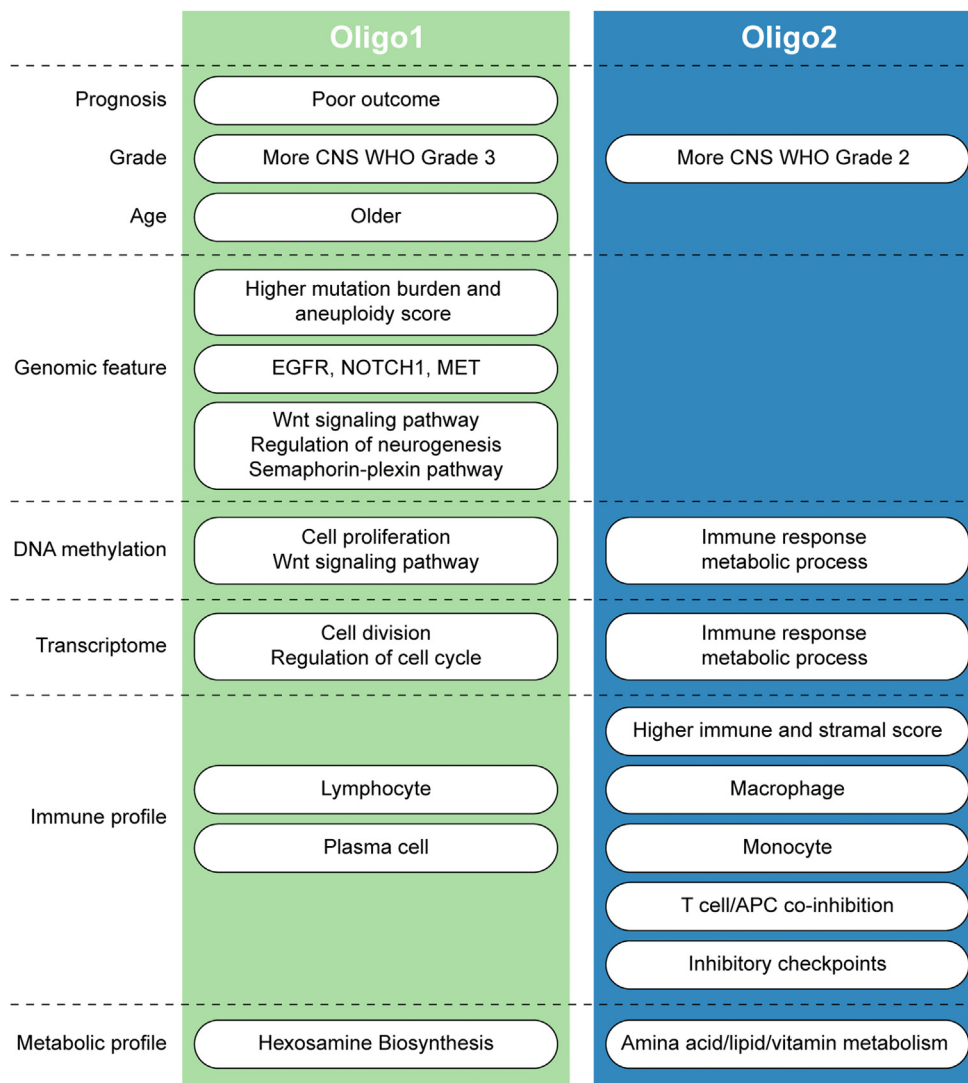
**Fig. 8: Overview of immune subtypes of human oligodendrogliomas.** We identified two expression-based subgroups in oligodendrogliomas, and the clinical characteristics, somatic variations, DNA methylation data, transcriptional data, immune infiltration, and metabolic enrichments of these two immune subtypes were explored.

## Discussion

This study represented the largest multi-platform genomic analysis performed to date of oligodendrogliomas (CNS WHO grade 2 and 3). A simplified graphical summary of the identified subtypes and their main clinical and biological characteristics was showed in Fig. 8. Our study identified two expression-based subgroups in oligodendrogliomas and robustly reproduced this classification in two public datasets through unsupervised analysis of immune-related gene profiles. The clinical characteristics, somatic variations, DNA methylation data, transcriptional data, immune infiltration, and metabolic enrichments of these two immune subtypes were explored. Our findings extended the

molecular subtyping of oligodendrogliomas and deepened our knowledge of immune heterogeneity within this tumor.

The two acquired subtypes of oligodendrogliomas had different patterns of DNA alterations. Oligo1 tumors had a more aggressive histological and genomic profile with higher mutation burden. The frequently variated genes observed in Oligo1 tumors, such as *WNT2, SHH, WNT11, FZD1,* and *SOX17,* were involved in Wnt signaling pathway, which has been implicated in the malignant progression of oligodendrogliomas.[47] *EGFR* mutations, which are characteristic of approximately 40% of glioblastomas (GBMs) and contribute to glioma behavior,[48,49] were observed in 18%

of Oligo1 tumors. Besides, altered genes annotated to negative regulation of neurogenesis were frequently observed in Oligo1 tumors. Since evidence suggests that oligodendrogliomas originate in oligodendrocyte precursor cell (OPC),[50] which can differentiate into oligodendrocytes, astrocytes, and neural cells,[51] the differentiation capacity would be lost in Oligo1 tumors. In addition, genes involved in semaphoring-plexin pathway, known as key regulator of GBM cell growth and survival,[52–54] were significantly altered in Oligo1 group. Consistently, the DNA methylation and transcriptome expression changes in Oligo1 tumors displayed similar signal pathway enrichments, such as Wnt signaling pathway (Supplementary Fig. S4). These findings suggest that Oligo1 tumors might be candidates for therapeutic strategies aiming at Wnt signaling, *EGFR*, differentiation or semaphorin-plexin pathway, which needs further exploration and investigation.

Despite several immunotherapeutic approaches, such as checkpoint blockade, cytokine therapy, cellular therapy, and vaccines, have been proven to work well in treating many malignant cancers,[55,56] immunotherapeutic modalities yield limited success in gliomas. *CTLA-4* and *PD-1* inhibitors have failed in clinical trials of gliomas.[57] *EGFR*vIII-targeted peptide vaccine (Rindopepimut) displays no significant improvement in median OS of GBM patients.[58] A comprehensive understanding of tumor immune microenvironment and precise immune subtyping are critical for improving the efficacy of current immunotherapies. Through several immune-related tools, we enquired the immune infiltration of two immune subtypes. Oligo2 group showed higher levels of immune, stromal scores, and myeloid cells, as well as increased functions of APC and T-cell co-inhibition. Moreover, Oligo2 tumors highly expressed several inhibitive checkpoint genes, such as *TIGIT, HAVCR2, LAIR1, LGALS9, PDCD1LG2,* and *C10orf54.* These findings suggest that the TME of Oligo2 tumors is highly immunosuppressive, and immunotherapies targeting at inhibitive checkpoints might be effective in this tumor subtype.

It is increasingly clear that tumors have heterogeneous metabolic preferences and dependencies. Within the given tumor, cancer cells display various metabolic pathway enrichments.[59,60] In addition to the well-known Warburg effect, growing evidence reveals that glutamine, fatty acids, and ketones can be utilized by cancer cells through tricarboxylic acid cycle (TCA) or mitochondrial oxidative phosphorylation.[61,62] Besides, several metabolic pathways are significantly correlated with clinical outcome and have potential prognostic value. Carbohydrate and nucleotide metabolism, for instance, are associated with poor prognosis, whereas TCA and lipid metabolism imply better outcome.[63,64] Consistently, Oligo2 tumors, exhibiting higher levels of metabolism involved in lipids, had favorable outcome. Oligo1 patients, with poor outcome, are significantly associated

with high level of hexosamine biosynthesis pathway (HBP). HBP, a shunt pathway of glycolysis, is a metabolic node in cancer cells that can promote survival.[65,66] Targeting HBP might be a potential therapeutic vulnerability in Oligo1 tumors.

Growing studies show that metabolic heterogeneity with the tumor environment influences the local immune cell function and might lead to immunotherapy failures. For example, lactate derived from cancer cells inhibits T-cell and NK-cell function and suppresses monocyte activation and differentiation of dendritic cells.[67,68] Cancer cells will suppress T-cell activation by excessive consumption of nutrients, inhibition of glucose and glutamine will impair T-cell proliferation and function.[69,70] Here, Oligo2 tumors, with higher scores of metabolism processes that were related to amino acid, lipids, and vitamin, showed increased functions of APC and T-cell co-inhibition. These results implied potential correlation between the specific metabolism processes and T-cell function, which required to be studied further.

In order to reveal the association between genomic alterations and immune infiltration which differed in these two subtypes, we performed in vitro and in vivo assays using *EGFR* and *MET* inhibitors. Our results showed that *EGFR* and *MET* inhibition in glioblastoma cells reduced T-cell migration but increased monocyte migration. Unfortunately, we lacked oligodendroglioma cell lines to further validate our bioinformatic findings, since this cell lines were unavailable and difficult to establish. Moreover, the molecular mechanism of *EGFR* and *MET* regulation on T cell and monocyte migration remains unclear and needs to be further explored. Performing secretomic analysis might help us reveal the potential regulatory mechanism.

In summary, our study introduced a new immune classification in oligodendrogliomas, which comprised two robust clusters with distinct prognosis, somatic variation, immune infiltration, and metabolic phenotype. Further investigation of this immune classifier in a larger cohort of patients is needed to determine its potential use as predictive biomarker.

**Appendix A. Supplementary data**

Supplementary data related to this article can be found at https://doi.org/10.1016/j.ebiom.2022.104410.

**References**

1 Louis DN, Perry A, Reifenberger G, et al. The 2016 World Health Organization classification of tumors of the central nervous system: a summary. *Acta Neuropathol.* 2016;131(6):803–820.

2 Louis DN, Perry A, Wesseling P, et al. The 2021 WHO classification of tumors of the central nervous system: a summary. *Neuro Oncol.* 2021;23(8):1231–1251.

3 Wesseling P, van den Bent M, Perry A. Oligodendroglioma: pathology, molecular mechanisms and markers. *Acta Neuropathol.* 2015;129(6):809–827.

4 Bou Zerdan M, Assi HI. Oligodendroglioma: a review of management and pathways. *Front Mol Neurosci.* 2021;14:722396.

5 Cancer Genome Atlas Research N, Brat DJ, Verhaak RG, et al. Comprehensive, integrative genomic analysis of diffuse lower-grade gliomas. *N Engl J Med.* 2015;372(26):2481–2498.

6 So J, Mamatjan Y, Zadeh G, Aldape K, Moraes FY. Transcription factor networks of oligodendrogliomas treated with adjuvant radiotherapy or observation inform prognosis. *Neuro Oncol.* 2021;23(5):795–802.

7 Labreche K, Simeonova I, Kamoun A, et al. TCF12 is mutated in anaplastic oligodendroglioma. *Nat Commun.* 2015;6:7207.

8 Aihara K, Mukasa A, Nagae G, et al. Genetic and epigenetic stability of oligodendrogliomas at recurrence. *Acta Neuropathol Commun.* 2017;5(1):18.

9 Tirosh I, Venteicher AS, Hebert C, et al. Single-cell RNA-seq supports a developmental hierarchy in human oligodendroglioma. *Nature.* 2016;539(7628):309–313.

10 Kamoun A, Idbaih A, Dehais C, et al. Integrated multi-omics analysis of oligodendroglial tumours identifies three subgroups of 1p/19q co-deleted gliomas. *Nat Commun.* 2016;7:11263.

11 Thorsson V, Gibbs DL, Brown SD, et al. The immune landscape of cancer. *Immunity.* 2018;48(4):812–830.e4.

12 Li B, Cui Y, Nambiar DK, Sunwoo JB, Li R. The immune subtypes and landscape of squamous cell carcinoma. *Clin Cancer Res.* 2019;25(12):3528–3537.

13 Sia D, Jiao Y, Martinez-Quetglas I, et al. Identification of an immune-specific class of hepatocellular carcinoma, based on molecular features. *Gastroenterology.* 2017;153(3):812–826.

14 He Y, Jiang Z, Chen C, Wang X. Classification of triple-negative breast cancers based on Immunogenomic profiling. *J Exp Clin Cancer Res.* 2018;37(1):327.

15 Wu F, Wang ZL, Wang KY, et al. Classification of diffuse lower-grade glioma based on immunological profiling. *Mol Oncol.* 2020;14(9):2081–2095.

16 Luoto S, Hermelo I, Vuorinen EM, et al. Computational characterization of suppressive immune microenvironments in glioblastoma. *Cancer Res.* 2018;78(19):5574–5585.

17 Bockmayr M, Klauschen F, Maire CL, et al. Immunologic profiling of mutational and transcriptional subgroups in pediatric and adult high-grade gliomas. *Cancer Immunol Res.* 2019;7(9):1401–1411.

18 Xu S, Tang L, Li X, Fan F, Liu Z. Immunotherapy for glioma: current management and future application. *Cancer Lett.* 2020;476:1–12.

19 Yang K, Wu Z, Zhang H, et al. Glioma targeted therapy: insight into future of molecular approaches. *Mol Cancer.* 2022;21(1):39.

20 Platten M, Bunse L, Wick A, et al. A vaccine targeting mutant IDH1 in newly diagnosed glioma. *Nature.* 2021;592(7854):463–468.

21 Bunse L, Rupp AK, Poschke I, et al. AMPLIFY-NEOVAC: a randomized, 3-arm multicenter phase I trial to assess safety, tolerability and immunogenicity of IDH1-vac combined with an immune checkpoint inhibitor targeting programmed death-ligand 1 in isocitrate dehydrogenase 1 mutant gliomas. *Neurol Res Pract.* 2022;4(1):20.

22 Ceccarelli M, Barthel FP, Malta TM, et al. Molecular profiling reveals biologically discrete subsets and pathways of progression in diffuse glioma. *Cell.* 2016;164(3):550–563.

23 Hu H, Mu Q, Bao Z, et al. Mutational landscape of secondary glioblastoma guides MET-targeted trial in brain tumor. *Cell.* 2018;175(6):1665–1678.e8.

24 Zhao Z, Zhang KN, Wang Q, et al. Chinese glioma genome Atlas (CGGA): a comprehensive resource with functional genomic data from Chinese glioma patients. *Genom Proteom Bioinformatics.* 2021;19(1):1–12.

25 Charoentong P, Finotello F, Angelova M, et al. Pan-cancer immunogenomic analyses reveal genotype-immunophenotype relationships and predictors of response to checkpoint blockade. *Cell Rep.* 2017;18(1):248–262.

26 Gentles AJ, Newman AM, Liu CL, et al. The prognostic landscape of genes and infiltrating immune cells across human cancers. *Nat Med.* 2015;21(8):938–945.

27 Wilkerson MD, Hayes DN. ConsensusClusterPlus: a class discovery tool with confidence assessments and item tracking. *Bioinformatics.* 2010;26(12):1572–1573.

28 Wu F, Chai RC, Wang Z, et al. Molecular classification of IDH-mutant glioblastomas based on gene expression profiles. *Carcinogenesis.* 2019;40(7):853–860.

29 Tibshirani R, Hastie T, Narasimhan B, Chu G. Diagnosis of multiple cancer types by shrunken centroids of gene expression. *Proc Natl Acad Sci USA.* 2002;99(10):6567–6572.

30 Wu F, Liu YW, Li GZ, et al. Metabolic expression profiling stratifies diffuse lower-grade glioma into three distinct tumour subtypes. *Br J Cancer.* 2021;125(2):255–264.

31 Kapp AV, Tibshirani R. Are clusters found in one dataset present in another dataset? *Biostatistics.* 2007;8(1):9–31.

32 Newman AM, Liu CL, Green MR, et al. Robust enumeration of cell subsets from tissue expression profiles. *Nat Methods.* 2015;12(5):453–457.

33 Wu F, Li GZ, Liu HJ, et al. Molecular subtyping reveals immune alterations in IDH wild-type lower-grade diffuse glioma. *J Pathol.* 2020;251(3):272–283.

34 Yoshihara K, Shahmoradgoli M, Martinez E, et al. Inferring tumour purity and stromal and immune cell admixture from expression data. *Nat Commun.* 2013;4:2612.

35 Hanzelmann S, Castelo R, Guinney J. GSVA: gene set variation analysis for microarray and RNA-seq data. *BMC Bioinformatics.* 2013;14:7.

36 Yang C, Huang X, Liu Z, Qin W, Wang C. Metabolism-associated molecular classification of hepatocellular carcinoma. *Mol Oncol.* 2020;14(4):896–913.

37 Rosario SR, Long MD, Affronti HC, et al. Pan-cancer analysis of transcriptional metabolic dysregulation using the Cancer Genome Atlas. *Nat Commun.* 2018;9(1):5330.

38 Huang R, Li G, Wang Z, et al. Identification of an ATP metabolism-related signature associated with prognosis and immune microenvironment in gliomas. *Cancer Sci.* 2020;111(7):2325–2335.

39 Huang da W, Sherman BT, Lempicki RA. Systematic and integrative analysis of large gene lists using DAVID bioinformatics resources. *Nat Protoc.* 2009;4(1):44–57.

40 Mermel CH, Schumacher SE, Hill B, et al. GISTIC2.0 facilitates sensitive and confident localization of the targets of focal somatic copy-number alteration in human cancers. *Genome Biol.* 2011;12(4):R41.

41 Wu F, Zhang C, Cai J, et al. Upregulation of long noncoding RNA HOXA-AS3 promotes tumor progression and predicts poor prognosis in glioma. *Oncotarget.* 2017;8(32):53110–53123.

42 Garofano L, Migliozzi S, Oh YT, et al. Pathway-based classification of glioblastoma uncovers a mitochondrial subtype with therapeutic vulnerabilities. *Nat Cancer.* 2021;2(2):141–156.

43 Zhang C, Cheng W, Ren X, et al. Tumor purity as an underlying key factor in glioma. *Clin Cancer Res.* 2017;23(20):6279–6291.

44 Wang Q, Hu B, Hu X, et al. Tumor evolution of glioma-intrinsic gene expression subtypes associates with immunological changes in the microenvironment. *Cancer Cell.* 2018;33(1):152.

45 Zarour HM. Reversing T-cell dysfunction and exhaustion in cancer. *Clin Cancer Res.* 2016;22(8):1856–1864.

46 Gonzalez-Gugel E, Saxena M, Bhardwaj N. Modulation of innate immunity in the tumor microenvironment. *Cancer Immunol Immunother.* 2016;65(10):1261–1268.

47 Chen HL, Chew LJ, Packer RJ, Gallo V. Modulation of the Wnt/beta-catenin pathway in human oligodendroglioma cells by Sox17 regulates proliferation and differentiation. *Cancer Lett.* 2013;335(2):361–371.

48 Horbinski C, Hobbs J, Cieply K, Dacic S, Hamilton RL. EGFR expression stratifies oligodendroglioma behavior. *Am J Pathol.* 2011;179(4):1638–1644.

49 Eskilsson E, Rosland GV, Solecki G, et al. EGFR heterogeneity and implications for therapeutic intervention in glioblastoma. *Neuro Oncol.* 2018;20(6):743–752.

50 Persson AI, Petritsch C, Swartling FJ, et al. Non-stem cell origin for oligodendroglioma. *Cancer Cell.* 2010;18(6):669–682.

51 Tsoa RW, Coskun V, Ho CK, de Vellis J, Sun YE. Spatiotemporally different origins of NG2 progenitors produce cortical interneurons versus glia in the mammalian forebrain. *Proc Natl Acad Sci U S A.* 2014;111(20):7444–7449.

52 Angelucci C, Lama G, Sica G. Multifaceted functional role of semaphorins in glioblastoma. *Int J Mol Sci.* 2019;20(9).

53 Angelopoulou E, Piperi C. Emerging role of plexins signaling in glioma progression and therapy. *Cancer Lett.* 2018;414:81–87.

54 Li X, Law JW, Lee AY. Semaphorin 5A and plexin-B3 regulate human glioma cell motility and morphology through Rac1 and the actin cytoskeleton. *Oncogene.* 2012;31(5):595–610.

55 Del Paggio JC. Immunotherapy: cancer immunotherapy and the value of cure. *Nat Rev Clin Oncol.* 2018;15(5):268–270.

56 Christofi T, Baritaki S, Falzone L, Libra M, Zaravinos A. Current perspectives in cancer immunotherapy. *Cancers (Basel).* 2019;11(10).

57 Schalper KA, Rodriguez-Ruiz ME, Diez-Valle R, et al. Neoadjuvant nivolumab modifies the tumor immune microenvironment in resectable glioblastoma. *Nat Med.* 2019;25(3):470–476.

58 Weller M, Butowski N, Tran DD, et al. Rindopepimut with temozolomide for patients with newly diagnosed, EGFRvIII-expressing glioblastoma (ACT IV): a randomised, double-blind, international phase 3 trial. *Lancet Oncol.* 2017;18(10):1373–1385.

59 Sonveaux P, Vegran F, Schroeder T, et al. Targeting lactate-fueled respiration selectively kills hypoxic tumor cells in mice. *J Clin Invest.* 2008;118(12):3930–3942.

60 Whitaker-Menezes D, Martinez-Outschoorn UE, Flomenberg N, et al. Hyperactivation of oxidative mitochondrial metabolism in epithelial cancer cells in situ: visualizing the therapeutic effects of metformin in tumor tissue. *Cell Cycle.* 2011;10(23):4047–4064.

61 Bonuccelli G, Tsirigos A, Whitaker-Menezes D, et al. Ketones and lactate "fuel" tumor growth and metastasis: evidence that epithelial cancer cells use oxidative mitochondrial metabolism. *Cell Cycle.* 2010;9(17):3506–3514.

62 Fan J, Kamphorst JJ, Mathew R, et al. Glutamine-driven oxidative phosphorylation is a major ATP source in transformed mammalian cells in both normoxia and hypoxia. *Mol Syst Biol.* 2013;9:712.

63 Peng X, Chen Z, Farshidfar F, et al. Molecular characterization and clinical relevance of metabolic expression subtypes in human cancers. *Cell Rep.* 2018;23(1):255–269.e4.

64 Kim J, DeBerardinis RJ. Mechanisms and implications of metabolic heterogeneity in cancer. *Cell Metab.* 2019;30(3):434–446.

65 Lam C, Low JY, Tran PT, Wang H. The hexosamine biosynthetic pathway and cancer: current knowledge and future therapeutic strategies. *Cancer Lett.* 2021;503:11–18.

66 Kim J, Lee HM, Cai F, et al. The hexosamine biosynthesis pathway is a targetable liability in KRAS/LKB1 mutant lung cancer. *Nat Metab.* 2020;2(12):1401–1412.

67 Brand A, Singer K, Koehl GE, et al. LDHA-associated lactic acid production blunts tumor immunosurveillance by T and NK cells. *Cell Metab.* 2016;24(5):657–671.

68 Gottfried E, Kunz-Schughart LA, Ebner S, et al. Tumor-derived lactic acid modulates dendritic cell activation and antigen expression. *Blood.* 2006;107(5):2013–2021.

69 Macintyre AN, Gerriets VA, Nichols AG, et al. The glucose transporter Glut1 is selectively essential for CD4 T cell activation and effector function. *Cell Metab.* 2014;20(1):61–72.

70 Johnson MO, Wolf MM, Madden MZ, et al. Distinct regulation of Th17 and Th1 cell differentiation by glutaminase-dependent metabolism. *Cell.* 2018;175(7):1780–1795.e19.